ACS APPLIED MATERIALS & INTERFACES

Research Article

www.acsami.org

Surface State of Sacrificial Copper Electrode by Electropolishing in Hydrophobic Ionic Liquid 1-Butyl-3-methylimidazolium bis(trifluoromethylsulfonyl)imide

Olga Lebedeva,[†] Gilyana Dzhungurova,[†] Alexandre Zakharov,[†,*] Dmitry Kultin,[†] Leonid Kustov,[†,‡] Vladimir Krasovskii,[‡] Konstantin Kalmykov,[†] and Sergey Dunaev[†]

[†]Department of Chemistry, Lomonosov Moscow State University, 119991 Moscow, Russia

[‡]Zelinsky Institute of Organic Chemistry, Leninsky Prospect 47, 119991 Moscow, Russia

Supporting Information

ABSTRACT: Anodic dissolution of natural surface-oxidized, air-annealed, cathodically reduced, and cathodically deposited copper in hydrophobic ionic liquid 1-buthyl-3-methylimidazolium bis(trifluoromethylsulfonyl)imide under galvanostatic conditions by means of gravimetric measurements was studied. The resulting samples were mirror-like oxide-free copper pattern. The mechanism of the electropolishing of oxidized copper surface was considered. The consequent anodic reactions $Cu_2O - 1e = Cu^+ + CuO$, $CuO - 2e = Cu^{2+} + O$, and $Cu - 1e = Cu^+$ take place. The electropolishing itself occurs over oxygen-free copper surface due to competitive residual water discharge in the pits and copper dissolution on the roughness.

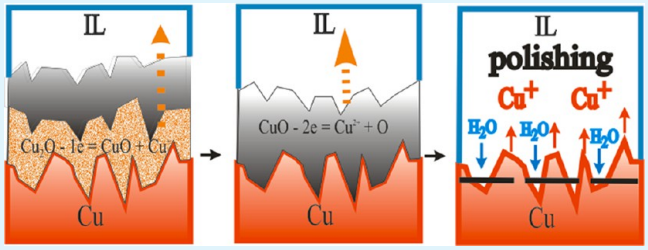

KEYWORDS: *ionic liquids, copper, electrochemistry*

INTRODUCTION

It is of no surprise that properties of metals essentially depend on the state of its surface. The most important metals to use as constructive materials, electrical conductors, and instruments are usually surface-oxidized in air. Oxide films provide protection from chemical or electrochemical corrosion but generally deteriorate useful properties of metals.

Usually metallic copper is covered with thin oxide film, Cu_2O, which, to a certain extent, protect the metal from corrosion. However, in recent years, growing attention was paid to the problem of chemical removal of surface oxides. Electropolishing of metals is of outstanding importance in a lot of industrial sectors. There are numerous examples indicating that the result of the metal electropolishing is directly connected with the features of polishing electrolyte solutions.

Electrochemical behavior of copper was studied well enough in aqueous solutions.[1] In contrast, data referred to ionic liquids as electrolytes are yet extremely poor. Nevertheless, ionic liquids are of greater interest as electrolytes for electropolishing of wide set of metals due to its electroconductivity and noticeable electrochemical stability (electrochemical window).[2] Moreover, ionic liquids are considered to be green solvents rather water,[3] as its moderate electroconductivity allows using these solvents without harmful supporting electrolytes.

Ionic liquids based on imidazolium cation are reported to exhibit markedly anticorrosion properties with respect to copper in aqueous solutions.[1,4] Also, it is of growing interest to use ionic liquids particularly hydrophobic based on PF_6^-, $N(SO_2CF_3)_2^-$ and others anions for electropolishing of metals.

Electrochemical behavior of copper with different surface state in ionic liquids is yet ambiguous enough. In the present study the features of the anodic dissolution of copper electrodes with different surface states in hydrophobic ionic liquid 1-buthyl-3-methylimidazolium bis(trifluoromethylsulfonyl)imide were investigated.

EXPERIMENTAL SECTION

Materials and Samples. For electrochemical measurements, copper foils (99.99%) were used as plates (25 × 5 × 0.3 mm): nature surface oxidized (NSO) copper, air-annealed copper, cathodically-reduced copper, and cathodically-deposited copper. Hydrophobic ionic liquid 1-buthyl-3-methylimidazolium bis(trifluoromethylsulfonyl)imide ($BmimNTf_2$) was used as purchased from Merck, Germany.

Water-saturated $BmimNTf_2$ was prepared as follows: 2 mL of ionic liquid and 2 mL of deionized water were shaken for 10 min at room temperature and allowed standing for 2 h to separate layers.

NSO Copper Electrode. The samples of copper foils obtained by cutting from NSO copper sheet were degreased with acetone and accurately dried.

Air-Annealed Copper Electrode. The copper foil firstly was treated with 20% hydrochloric acid for 15 min, washed with distilled water, and accurately dried. The etched foil of copper was annealed in oven

Received: June 7, 2013
Accepted: October 10, 2013
Published: October 10, 2013

   dx.doi.org/10.1021/am402213r | *ACS Appl. Mater. Interfaces* 2013, 5, 10551−10558

in air at 700 K for 10 s to prepare temper colors, cooled down to room temperature, degreased with acetone and dried in air.

Cathodically-Reduced Copper Electrode. Cathodically-reduced copper (CRC) anode was prepared by reduction in $BMImNTf_2$ for 15 min at cathodic current density of 6−8 $mA{\cdot}cm^{-2}$. Then the polarities of electrodes were changed without taking out from electrolyte.

Deposited Copper Electrode. Before copper electrodeposition the copper foil was immersed into 20% hydrochloric acid and after 15 min washed with distilled water. The electrodeposition of copper upon copper cathode was performed by electrolysis with sacrificial copper anode from aqueous $CuSO_4$ solution at i = 10 $mA{\cdot}cm^{-2}$ for 1 h.

Products of the anodic dissolution of copper in $BmimNTf_2$ were centrifuged, washed with acetone and distilled water, and dissolved in HNO_3. Copper in the solution obtained was determined volumetrically by iodometric titration.

Electrochemical Measurements. Two- and three-electrode cells with unseparated compartments were used. The volume of ionic liquids was 3−4 mL. The working and auxiliary electrodes were Cu foil (0.3 mm in thickness). The working surface of the electrode was 0.3−0.6 cm^2. The quasi-reference electrode was silver wire (0.5 mm in diameter). The distance between the working and auxiliary electrodes during polishing was 3−4 mm. The experiments were all carried out at room temperature (25 °C) in air.

Cyclic voltammograms of Cu were performed at room temperature in ionic liquid at the potential scanning rate of 50 $mV{\cdot}s^{-1}$. The AUTOLAB PGSTAT 302N potentiostat/galvanostat was used. Anodic dissolution of copper was carried out under galvanostatic conditions (the current density was within 6-8 $mA{\cdot}cm^{-2}$).

The gravimetric experiments were carried out using analytical balance KERN ABT220-4M. Electrodes were weighted before and after anodic treatment. The maximum deviation in the mass loss observed was 5%.

Scanning electron microscopy (SEM) measurements were carried out by means of EVO-50 "Zeiss" techniques, EDX analyzer.

RESULTS AND DISCUSSION

Effect of surface state upon electrochemical properties of copper was studied by means of cyclic voltammetry (CV) in $BmimNTf_2$ at room temperature. Two samples of copper electrode with different surface state were selected. The first one was a mirror-bright electrode prepared by electropolishing of copper in $BmimNTf_2$. This electrode got smoothed oxide-free surface. The second one was prepared after exposition of electropolished copper electrode to air at room temperature for some days (NSO). The surface of the air-exposed pattern visually was also mirror-like as the first one.

CV of Copper Electrode in $BmimNTf_2$. There is unambiguous difference in electrochemical behavior of surface-oxidized and oxide-free copper in $BmimNTf_2$. Figure 1 performs CVs for both samples and platinum to compare. It's of no surprise that the surface-oxidized copper electrode doesn't exhibit any features within the first potential cycle of cyclic voltammogram (*1*). However, the second potential cycle reveals small peaks on anodic and cathodic scans (*2*). As the lower oxidation state of copper is known to be more stable in nonaqueous solutions,[5] these peaks may be attributed to irreversible reactions 1 and 1a, respectively, proceeding on oxide-free sites.

$$Cu - 1e \rightarrow Cu^{+}_{ad} \quad (1)$$

$$Cu^{+}_{ad} + 1e \rightarrow Cu \quad (1a)$$

As to the oxide-free copper electrode the anodic curve for the first potential cycle (*3*) seemed to exhibit two current peaks probably due to copper oxidation and residue water discharge

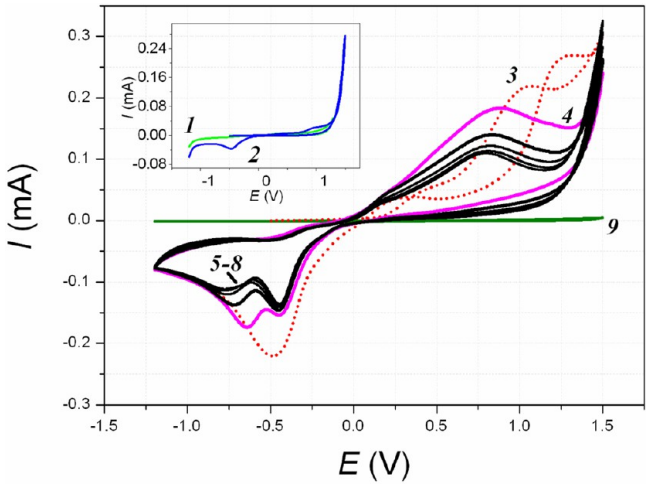

Figure 1. CV for the 1st and 2nd potential cycles of NSO copper electrode (*1* and *2*, respectively), for the 1st through 6th potential cycles of oxide-free copper electrode (*3*−*8*), and for Pt electrode (*9*) in dry $BmimNTf_2$ (potential scan rate is 50 $mV{\cdot}s^{-1}$).

on the smoothed oxide-free surface according to the reactions 1 and 2, respectively. Hydrophobic ionic liquid is known always to consist residue water.

$$H_2O - 2e = O_{ad} + 2H^{+} \quad (2)$$

The appearance of hysteresis on cathodic curve of the first potential cycle (Figure 1, curve 3) is probably connected with a partial modification of the surface of the copper electrode due to pitting corrosion.[6] The shape of the second potential cycle differs markedly the first one. As it is seen in Figure 1 (curve *4*), there is only single diffused peak current in anodic direction and two cathodic processes are registered. With the increase in the number of cycles (Figure 1, curves *3*−*8*) stabilization of surface occurs, that is demonstrated the steady-state processes on the surface.

According to the CV, it is evident that the surface state of copper electrode plays crucial role by anodic dissolution in ionic liquid $BmimNTf_2$. To understand the mechanism of copper electrode behavior under anodic polarization in $BmimNTf_2$, four copper electrodes with different state of the surface were sampled to study under galvanostatic conditions.

NSO Copper Electrode. NSO copper is usually covered with thin layers of Cu_2O and CuO that efficiently protect copper from atmospheric corrosion at room temperature in the absence of moisture and CO_2. The copper oxide films are noticeable semiconductive and take part in electrochemical processes. It was found that the NSO copper electrode get effectively polished by anodic polarization in $BmimNTf_2$ medium.

Figure 2 demonstrates the plot of the mass loss (m) of the NSO copper anode in $BmimNTf_2$ as a function of the quantity of electricity (Q) consumed. There are two differently sloped lines shifted along Q axis in Figure 2. The unambiguously reproducible segment on the plot (Figure 2, insertion) is observed within the region of 1.55−2.15 C. The slopes of the lines within intervals of 0−1.55 (I), 1.55−2.15 (II), and 2.15−6.0 C (III) were found to be 54.8, 41.8, and 49.2 $g{\cdot}mol^{-1}$, respectively, which is indicative of the complex mechanism of copper dissolution. The slope within transition region (41.8 $g{\cdot}mol^{-1}$) was determined tangentially at the inflection point.

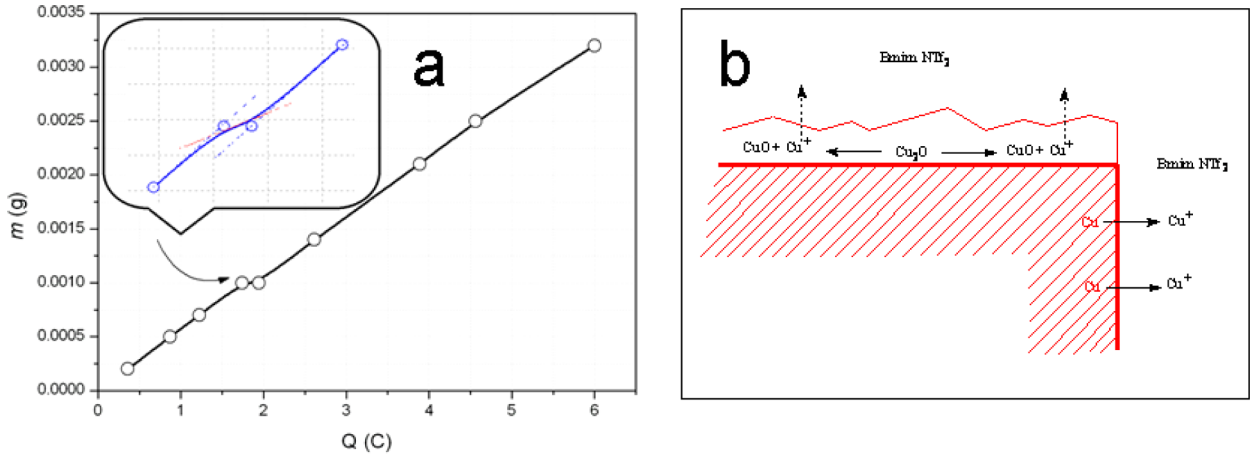

Figure 2. Plot of the mass loss of NSO copper anode as a function of quantity of electricity consumed in $BmimNTf_2$ (a) and scheme of the process (b).

The features observed on the $m-Q$ plot for NSO copper electrode in dry $BmimNTf_2$ leads to assumption that electropolishing mechanism includes three steps described by the lines above. The beginning of the copper anodic dissolution is probably connected with reaction 3 as the surface of the sample is covered with copper oxides.

$$Cu_2O - 1e = Cu^+ + CuO \quad (3)$$

However, O_2 evolution was observed at the start of the process. The oxygen evolution proceeded as if there were oxide-free sites upon the surface of the copper electrode. In fact, earlier,[7] we found that residual water in $BmimNTf_2$ does discharge on the etched copper electrode. The NSO sample was obtained by cutting of copper sheet so that the oxygen-free sites on the surface geometrically comprised about 10% of the total working areas.

Otherwise, it is reasonable to take into account the reaction 1 to proceed also on the oxide-free sites of the copper electrode. However, the expected slope of the plot corresponding to the competitive reactions 1 and 3 within 1.55−2.15 C region doesn't fit the slope of the plot observed (41.8 g·mol^{-1}). Also, the contribution of two-electron process ($Cu_2O - 2e = Cu^{+2} + CuO$) may be neglected because only traces of copper(II) species were found in $BmimNTf_2$.

The residual water present in hydrophobic ionic liquid $BmimNTf_2$ inhibits copper dissolution due to simultaneous water discharge according to the reaction 2. The data presented are agreed also with the results obtained for water inhibiting action by anodic dissolution of copper in other nonaqueous solutes, for example, in ethanolic solutions.[8]

Within the transition region, the reaction 4 is probable to occur followed by the reaction 2 proceeding on the oxide-free surface of the copper electrode.

$$CuO - 2e = Cu^{2+} + O_{ad} \quad (4)$$

As soon as CuO was consumed in the reaction 4, the slope of the plot quietly increases. By this moment (region III) the surface of the copper electrode is cleaned from oxides and the reaction 1 starts. However, only the reaction 1 is obviously to provide no slope observed (49.2 g·mol^{-1}). So, the competition of the reactions 1 and 2 probably takes place.

Despite the fact that no reaction 2 attributes to the mass loss of the copper electrode the linear dependence of m on Q is observed. It implies that the ratio Q_2/Q_1, where Q_1 and Q_2 are quantity of electricity consumed in the reactions 1 and 2, respectively, is constant.

Provided $Q_2/Q_1 = \alpha_1$ and $Q = Q_1 + Q_2$ the total quantity of electricity consumed is $Q = (1 + \alpha_1)Q_1$. In this case, the mass loss of the copper electrode may be expressed by means of the eq 5

$$m = M_{Cu}Q_1/zF \quad \text{or} \quad m = M_{Cu}Q/zF(1 + \alpha_1) \quad (5)$$

where M_{Cu} is molar mass of copper, F is Faraday's constant, and $z = 1$.

On the other hand, it was found experimentally that there is a linear relationship between m and Q (Figure 2, region III)

$$m = K_1Q \quad (6)$$

where Q is the total electricity consumed and K_1 is empirical constant, which is 49.2/F gC^{-1}.

A comparison of the eqs 5 and 6 gives

$$K_1 = M_{Cu}/(1 + \alpha_1)F \quad \text{and} \quad \alpha_1 = 0.29$$

Supposing no ratio Q_2/Q_1 changes where the reactions 1 and 2 compete, let's consider the region I of 0−1.55 C in which the copper mass loss is due to the reactions 1 and 3 accompanied by the reaction 2. The copper mass loss can be determined by means of the eq 7:

$$m = m_1 + m_3 = 54.8Q/F \quad (7)$$

where m_1 and m_3 are the mass losses due to the reactions 1 and 3, respectively, and Q is total quantity of electricity consumed. Equation 7 can be rewritten as

$$63.5(Q_1 + Q_3) = 54.8Q \quad (8)$$

where Q_1 and Q_3 are the quantity of electricity consumed in the reactions 1 and 3, respectively.

The linear relationship between the copper mass loss and Q in this region is possible if the ratio Q_3/Q_1 is constant. Designated Q_3/Q_1 as α_2 one can obtain $Q = Q_1 + Q_2 + Q_3 = Q_1(1 + \alpha_1 + \alpha_2)$. Then, eq 8 will be as follows:

$$63.5Q_1(1 + \alpha_2) = 54.7Q_1(1 + \alpha_1 + \alpha_2) \quad \text{and}$$

$$\alpha_2 = 0.81$$

Table 1. Electrodissolution of NSO Copper by Anodic Treatment in $BmimNTf_2$ within Intervals I–III[a]

			Q_i (C)							Δm (mg)	
region	p (g·mol^{-1})	Q (C)	Q_1	Q_2	Q_3	Q_4	α_1	α_2	α_3	obs.	calc.
I	54.8	0–1.55	0.73	0.21	0.60		0.29	0.83		0.880	0.875
II	41.8	1.55–2.15	0.10	0.29		0.48	0.29		4.8	0.260	0.264
III	49.2	2.15–6.0	2.98	0.86			0.29				

[a] $p = KF$ is slope of the plot (F is Faraday's constant); Q and Q_i are total and partial quantity of electricity consumed in corresponding reaction; α_1, α_2, and α_3 are ratios Q_2/Q_1, Q_3/Q_1, and Q_4/Q_1, respectively; Δm are observed and calculated copper mass losses within corresponding intervals.

Within 1.55–2.15 C, the copper mass loss comprises 0.00026 g. It is reasonable to assume that the mass loss within this region is connected with the reactions 1 and 4 accompanied by the water discharge.

Considering that ratios $\alpha_1 = Q_2/Q_1 = 0.29$ and $Q_4/Q_1 = \alpha_3$ (Q_4 is electricity consumed in the reaction 4) are constant to provide a linear relationship between m and Q, one can obtain eq 9

$$M_{CuO}Q_4/2F + M_{Cu}Q_1/1F = 41.8Q/F \quad (9)$$

where M_{CuO} is molar mass of CuO. It gives $\alpha_3 = 4.8$.

Accordantly, electricity consumed in the reactions 1, 2, and 4 within region II are presented in Table 1. The data obtained allow estimating the copper mass loss within the region of 1.55–2.15 C. The result is $m = m_{CuO} + m_{Cu} = 2.6 \times 10^{-4}$ g, which is consistent with the experimental data (Table 1).

So, retardation of the change in the copper mass loss observed within 1.55–2.15 C is in accordance with the model proposed.

Provided that it requires 0.48 C for the CuO dissolution the apparent thickness (h) of the oxide film (Cu_2O or Cu_2O and CuO) could be estimated by eq 10 as follows:

$$h = M_{CuO}Q/(zF\rho_{CuO}S) \quad (10)$$

where M_{CuO}, Q, F, ρ_{CuO}, and S are CuO molar mass, electricity, Faraday's constant, CuO density, and anode surface area, respectively, and $z = 2$. Taking $\rho_{CuO} = 6.31$ g·cm^{-3} and S = 0.5 cm^2, the apparent thickness of the copper oxides on the NSO copper electrode is $h = 627$ nm.

The apparent thickness of the oxide film covering the NSO copper sample seemed to be the same order as the visible light wavelength that explained the just noticeable interference picture on the metal.

Air-Annealed Copper Electrode. To specify the mechanism proposed the copper anode was preliminarily exposed to air at 700 K for 10 s to produce more copper oxide films. This procedure should result in the formation of the micrometer films of the copper oxides. The sample obtained was temper colored due to Cu_2O and CuO oxide films, the first being the closest to the metal surface (Figure 3).

The plot of the mass loss of the sacrificial copper anode annealed in air as a function of the quantity of electricity consumed in hydrophobic ionic liquid $BmimNTf_2$ is depicted in Figure 4. The plot in Figure 4 is seen unambiguously to differ the plot obtained for the NSO copper electrode. In this case, the m–Q plot proved to reveal two breaking points (1.10 and 1.88 C) that are evidently indicative of a change in the dissolution mechanism. The slopes of intercepts on the plot are given in Table 2.

At the very beginning, the slope of the first section (63.7 g·mol^{-1}) is probably to indicate that the only reaction 3 occurs. The total surface of the sample is unambiguously covered with

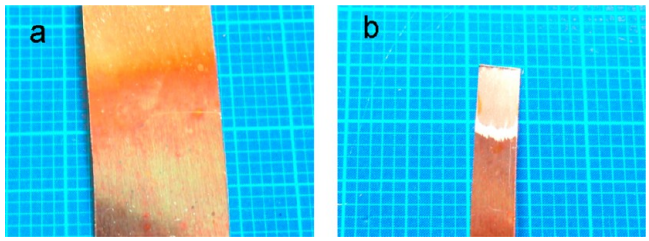

Figure 3. Photographs of the surface of air-annealed copper electrode before (a) and after (b) electropolishing in ionic liquid $BmimNTf_2$ (2.8 C).

copper oxide layers, which inhibit water discharge. It is reasonable to assume that the competition between the reactions 1 and 2 begins as soon as the oxide-free sites appear on the metal surface. The plot is clearly nonlinear. The change in Q_3/Q_1 ratio does be the dominant reason of nonlinearity of the plot.

Approximation to linearity gives opportunity to describe the observed plot as intersection of two lines (Figure 4) depicting the reaction 3 within the range of 0–1.10 C and the competition of the reactions 2 and 4 within the range of 1.10–1.88 C. The reaction 1 is ruled out also as for the above case with the NSO copper electrode. The slopes of these lines are presented in Table 2.

Thus, the closest layer, Cu_2O, is the first that takes part in the electro-oxidation process, and the dissolution of the copper electrode in the case of the annealed copper sample begins with the reaction 3.

After being consumed 1.10 C the slope of the plot decreases that may be connected with the competition of the reactions 4 and 2.

Considering the processes in this case (Supplemental Information) may obtain the data presented in Table 2.

Provided CuO uniformly covers the surface of the calcined copper electrode the apparent thickness of the oxide film may be calculated by means of eq 10. In the case of the annealed copper anode, as expected, the apparent thickness of the oxide film is noticeably greater than for the NSO copper (Table 2).

Over 1.88 C, the slope of the plot for the air-annealed copper electrode increases that is indicative of proceeding the reactions 1 and 2, as in the case of the NSO copper electrode. The slope obtained was 48.2 g·mol^{-1}. The Q_2/Q_1 ratio (α_1), where Q_1 and Q_2 are the electricity consumed in the reactions 1 and 2, respectively, was found to be equal to 0.32 (Table 2).

The mechanism of anodic behavior of air-exposed copper formulated by the reactions 1–4 is consistent with the kinetic data and changes in the surface state of the electrode (Figure 5).

Anodic Behavior of CRC Electrode. The results are supported by the plot of the mass loss of the copper anode obtained by preliminary cathodic treatment in $BmimNTf_2$

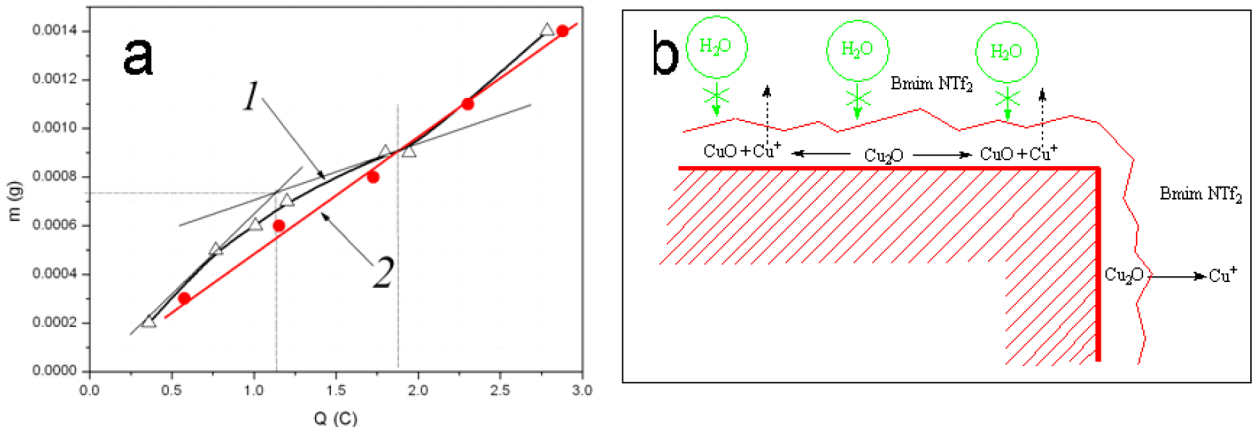

Figure 4. Plot of the copper mass loss versus quantity of electricity consumed by anodic treatment of the copper electrode obtained by preliminary exposition to air at 700 K for 10 s (*1*) and the plot of the mass loss for the CRC anode (*2*) in hydrophobic ionic liquid $BmimNTf_2$ (a) and scheme of the process (b).

Table 2. Observed and Calculated Slopes of the Plot of the Mass Loss for Air-Annealed Copper Electrode versus *Q*, Quantity of Electricity Consumed in Metal-Dependent Reaction (Q_i), $\alpha_4 = Q_2/Q_4$, $\alpha_1 = Q_2/Q_1$, Mass Loss (Δm), ρ is Density of Cu_2O and CuO, and Apparent Thickness of Oxide Layer (h) within Ranges I and II

			Q_i (C)				Δm (mg)				
	p (g·mol^{-1})	Q (C)	Q_1	Q_2	Q_3	Q_4	obs.	calc.	α_i	ρ (g·cm^{-3})	h (μm)
I	63.7	0–1.10			1.1		0.73	0.724		6.10	2.2
II	22.4	1.10–1.88		0.345		0.435	0.17	0.179	0.79	6.31	1.83
III	48.2	1.88–3.0	0.85	0.270					0.32		

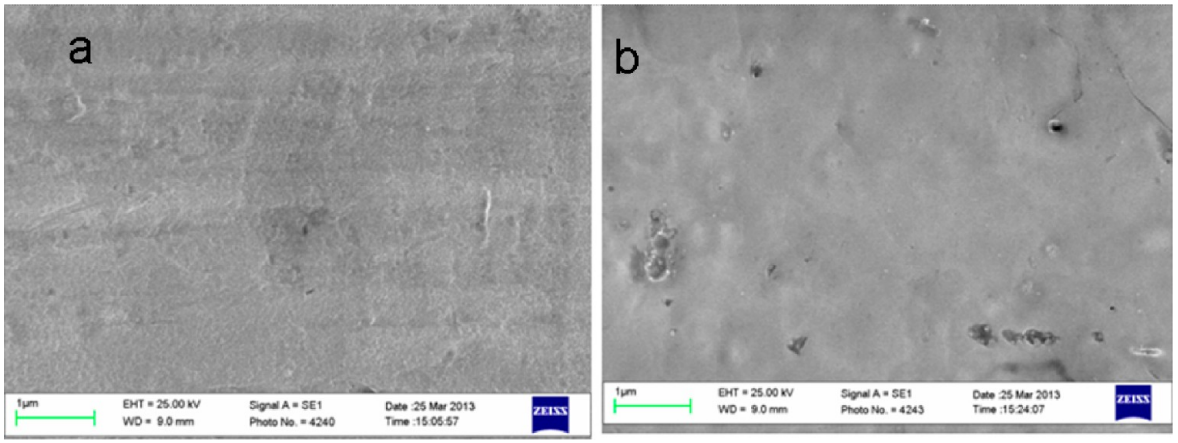

Figure 5. SEM images for air-exposed copper electrode before (a) and after (b) electropolishing in ionic liquid $BmimNTf_2$ (4.2 C).

versus the quantity of electricity. The plot of the mass loss of the CRC anode is also depicted in Figure 4. It is of interest that the plot slope in this case is much the same as for the oxidized copper electrode after dissolution of the oxide films (48.2 g·mol^{-1}).

The results obtained are also indicative of the competitive mechanism of the anodic dissolution of the copper electrode as soon as the oxide films are totally removed from the surface in ionic liquid $BmimNTf_2$ medium. The anode surface in this case is not only oxide-free but also smooth.

It should be noted that in the case of the CRC electrode the mass loss is linear-dependent on *Q* from the very beginning of the dissolution of copper (Figure 4). Moreover, the slope of the plot for the CRC electrode is the same as for copper electrode after the total removing of the oxides.

This phenomenon is explained by the assumption that the residual water discharge (reaction 2) in hydrophobic ionic liquids can proceed only on the oxide-free and smoothed surface of copper while for the reaction 1 such ≪selectivity≫ isn't observed.

Invariable slope of the *m*–*Q* plot for the CRC electrode under conditions of competition of reactions 1 and 2 also indicates that the ratio Q_2/Q_1 is constant all over the electropolishing of copper.

Using eqs 5 and 6 and the observed value of the plot slope for the CRC electrode, the Q_2/Q_1 ratio may be calculated. For this case, $\alpha_1 = 0.32$.

This result confirms that the anodic behavior of the copper electrode in hydrophobic ionic liquid $BmimNTf_2$ is strongly dependent on the surface state of the metal. In the case of smooth oxide-free surface of the copper electrode, the anodic

behavior of the metal depends also on the presence of water in hydrophobic ionic liquid.

Anodic Behavior of Copper Electrode Deposited from Aqueous Solution of $CuSO_4$ in $BmimNTf_2$. Smoothness or roughness of the surface also plays unambiguously important role in anodic behavior of the oxide-free copper electrode. Figure 6 illustrates the plot of the mass loss of the copper anode

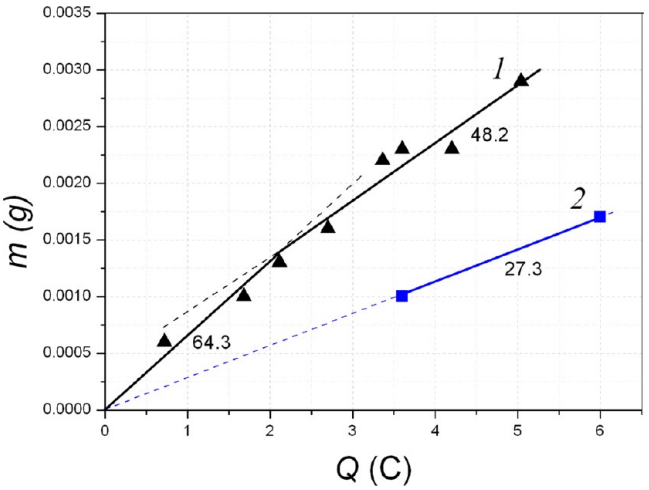

Figure 6. Plot of the mass loss for copper anode prepared via cathodic deposition of copper from aqueous solution of $CuSO_4$ versus quantity of electricity in dry (*1*) and water-saturated (*2*) $BmimNTf_2$.

prepared via cathodic deposition of copper from aqueous solution of $CuSO_4$. In this case, the surface of the electrode is covered in microcrystallites of metallic copper (Figure 7). The metal copper crystallites of this sample are seen to be far from smoothed but free of surface oxides.

There is a sharp difference between the plots presented in Figures 4 and 6 although there were no oxide films on the surface of both samples. For the CRC electrode (Figure 4), the plot of the mass loss of the copper electrode in $BmimNTf_2$ versus the quantity of electricity reveals no intersecting lines. It isn't the case for the plot depicted in Figure 6. Indeed, for the copper electrode obtained by electrodeposition from the aqueous solution of $CuSO_4$, two intersecting lines are observed. The slope of the first line seemed to be 64.3 $g \cdot mol^{-1}$, which was quite similar to the 63.5 $g \cdot mol^{-1}$ expected for the reaction 1. In respect, the electrode was prepared under conditions excluding oxide formation on the surface of the sample the process corresponding to this line is reasonable connected with the reaction 1. Reaction 1 is clear to lead to the electropolishing of roughness of the metallic copper crystallites formed by electrodeposition of copper from the aqueous solution of $CuSO_4$. SEM images presented in Figure 7 illustrate the change in the surface state of this copper electrode before and after anodic treatment in ionic liquid $BmimNTf_2$.

To begin with, the intersection point the slope of the $m-Q$ plot changes, which is undoubtedly subsequent upon a competition of the reactions 1 and 2, as for the case with the CRC electrode.

The change in the mechanism of the anodic dissolution of copper obtained by electrodeposition from the aqueous $CuSO_4$ solution and observed after intersection point is probably connected with the end of the electropolishing of the rough metal surface. Numerous observations indicate that the electrochemical reactions 1 and 2 effectively compete only on the smooth oxide-free copper surfaces as in the case presented in Figure 4 for the CRC electrode.

The tendency of copper atoms to the electro-oxidation via reaction 1 on the surface roughness in ionic liquid medium proved to be higher than water discharge at the same sites of the surface. This observation is suggested by the fact that gas evolution on the anode in this case appeared only through 10–20 min since the electrolysis was begun.

Earlier,[7] it was found that the reason of the retardation of copper electrochemical corrosion in hydrophobic ionic liquid $BmimNTf_2$ is due to water oxidation on smooth oxide-free surface of copper electrode. The contribution of the side-reaction of water oxidation to the slope of the plot of the copper mass loss increases with the increase in the H_2O concentration.

The increase in water concentration in ionic liquid $BmimNTf_2$ in case of copper deposited from $CuSO_4$ solution was found to lead to decrease in the slope of the mass loss plot (Figure 6, curve *2*). This observation is of no surprise. Earlier,[7] this feature was found for the etched copper anode. The plot of the mass loss for copper deposited from aqueous solution of

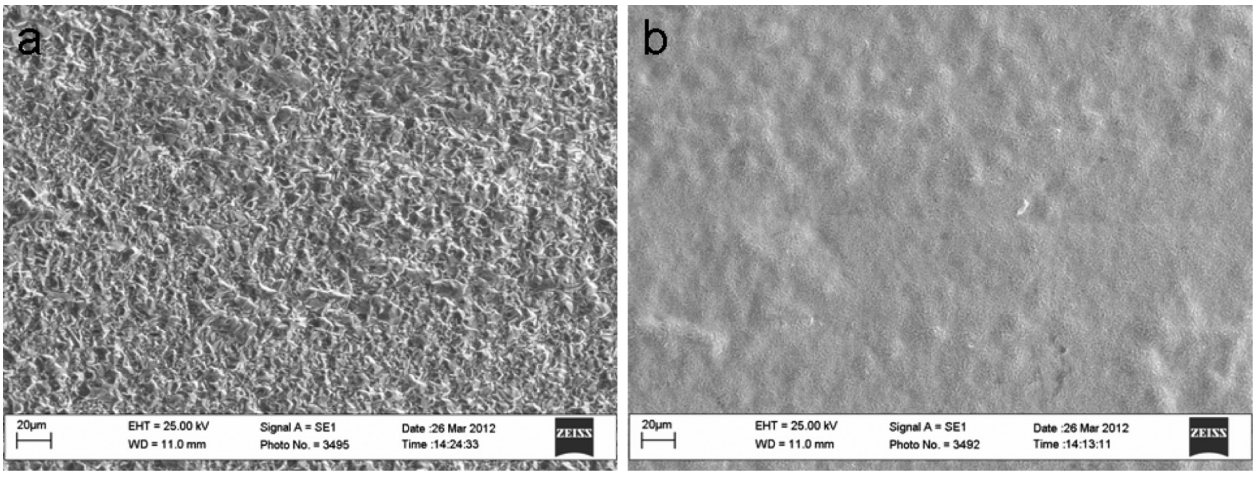

Figure 7. SEM images for the copper anode obtained via cathodic deposition of copper from aqueous solution of $CuSO_4$ before (a) and after (b) electropolishing in $BmimNTf_2$ (3.8 C).

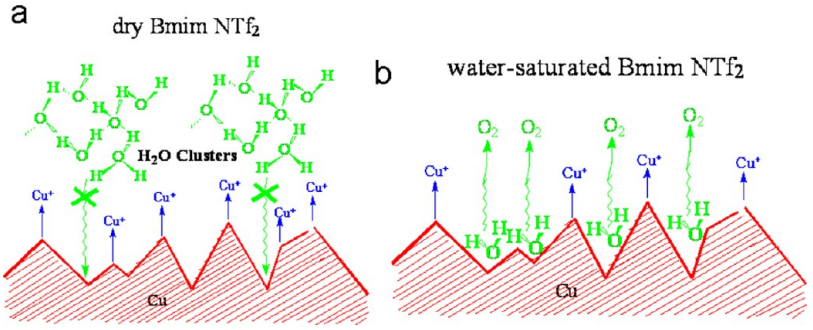

Figure 8. Scheme of electropolishing of rough copper electrode in dry (a) and in water-saturated (b) $BmimNTf_2$.

$CuSO_4$ has no intersection points in water-saturated ionic liquid $BmimNTf_2$. It is not the case for the dry ionic liquid $BmimNTf_2$ in which the dissolution of copper anode with rough surface reveals one intersection point.

Water is known to inhibit the anodic dissolution of copper[7] due to a tendency to discharge along with ionization of the copper atoms, which are oxidized on the roughness rather water molecules (Figure 8). The competitive tendency of water to discharge on anode enhances with the increase in water concentration.

The slope of the plot of the mass loss at the beginning is 64.3 $g{\cdot}mol^{-1}$ in the "dry" ionic liquid $BmimNTf_2$ that doubtless rules out the participation of water molecules in anodic process. However, to begin with, the intersection point the slope is the same as for the smooth and oxide-free CRC electrode (Figure 4). This result is indicative of the similarity in mechanisms of the anodic dissolution of cathodically-deposited from the aqueous $CuSO_4$ solution and CRC electrode.

Figure 6 (curve 2) plots also the mass loss of copper anode in water-saturated ionic liquid $BmimNTf_2$, which slope drops up to 27.3 $g{\cdot}mol^{-1}$ with respect to dry $BmimNTf_2$. By the assumption that the ratio $Q_2/Q_1 = \alpha_1$ is constant, one can calculate α_1 as above for the cathodically-deposited copper anode. Using eqs 5 and 6 the ratio α_1 was obtained $\alpha_1 = 1.33$. This result indicates that $Q_2 = 0.57Q$ and more than one half of the total quantity of electricity consumes in the reaction 2 in water-saturated ionic liquid $BmimNTf_2$.

Moreover, the data obtained show that the reaction 1 can effectively compete the water discharge only in "dry" ionic liquid $BmimNTf_2$. On the other hand, the presence of intersection on the plot of mass loss unambiguously implies that the discharge of water molecules is favored by smooth surface of the copper anode.

On the basis of the experimental data (Figure 6), the change in the mechanism of the anodic dissolution of copper having rough surface occurs at 2 C in "dry" ionic liquid $BmimNTf_2$. This result obviously can be considered as an estimation of time required for the electropolishing process.

It is obvious that electropolishing of copper having rough surface is favored by the presence of water in hydrophobic ionic liquid. The water molecules enforce the reaction 1 to proceed selectively on the sharp roughness of copper surface rather than in the pits, where copper ionization loses competition against water discharge due to water concentration increase. The increase in the water concentration favors the enhancement in ratio of small water clusters[9] capable to fill deep pits on the copper surface (Figure 8). This fact explains the absence of intersection point on the plot of the copper mass loss in water-saturated $BmimNTf_2$ (Figure 6). The filling of pits on the surface of copper electrode with water molecules by using water-saturated $BmimNTf_2$ inhibits the etching of copper and favors the decrease in time required for the copper electropolishing.

CONCLUSIONS

Surface state of sacrificial copper electrode unambiguously affects the anodic behavior of copper in hydrophobic ionic liquid $BmimNTf_2$. Copper oxide films are removed by the anodic treatment as insoluble thin powders of copper(I) oxide and as large minorities of Cu (II) compounds.

In all cases, after oxide films or roughness have been removed, the mass loss of the copper anode is clearly obeyed Faraday's law. The slopes of these plots seemed to be well correlated (Table 3), which is undoubtedly indicative of the similar mechanism of the electropolishing of the smoothed surfaces of the copper anodes due to the competitive reactions 1 and 2.

Table 3. Slopes of the Plots of the Mass Loss as a Function of Q for the Different Samples Obtained after Smoothing of the Copper Anodes by Electropolishing in Dry $BmimNTf_2$[a]

sample	slope ($g{\cdot}mol^{-1}$)	α_1
copper annealed in air	48.2	0.32
copper after electrochemical reduction	48.2	0.32
NSO copper	49.2	0.29
etched copper	50.1	0.27
copper catholically deposited from $CuSO_4$	47.8	0.33
average	48.7	0.31

[a] α_1 is ratio Q_2/Q_1, see text.

Also, it is of practical interest that the copper loss in these processes is minimized in water-rich $BmimNTf_2$, where the reaction 1 is inhibited by the water discharge. Under these conditions, the reaction 1 occurs on the highest sites of the roughness rather in pits where water molecules are mainly discharged.

ASSOCIATED CONTENT

Supporting Information

Equations 11 and 12. SEM images of samples prepared by different methods. This material is available free of charge via the Internet at http://pubs.acs.org.

AUTHOR INFORMATION

Corresponding Author

*E-mail: zakh-alex@yandex.ru.

Notes

The authors declare no competing financial interest.

REFERENCES

(1) Scendo, M.; Uznanska, J. *Int. J. Corrosion* **2011**, *2011*, 1−13. Kinoshita, K.; Landolt, D.; Muller, R. H.; Tobias, C. W. *J. Electrochem. Soc.* **1970**, *117* (10), 1246−1251. Li, G.; Camaioni, D. M.; Amonette, J. E. *J. Phys. Chem. B* **2010**, *114*, 12614−12622. Gimenez-Romero, D.; Garcia-Jareño, J. J.; Agrisuelas, J.; et al. *J. Phys. Chem. C* **2008**, *112*, 4275−4280. Li, D.; Xia, G.; Zheng, Z.; et al. *Int. J. Electrochem. Sci.* **2013**, *8*, 1041−1046.

(2) Zhao, H. *Chem. Eng. Commun.* **2006**, *193* (12), 1660−1677. Zhang, S.; Sun, N.; Xe, X.; Lu, X.; Zhang, X. *J. Phys. Chem. Ref. Data* **2006**, *35* (4), 1475−1517. Fernicola, A.; Scrosati, B.; Ohno, H. *Ionics* **2006**, *12* (2), 95−102. Tsuda, T.; Hussey, C. L. *Electrochem. Soc. Interface* **2007**, *16* (1), 42−49.

(3) Abbott, A. P.; Frish, G.; Hartley, J.; Rider, K. S. *Green Chem.* **2011**, *13*, 471−481.

(4) Gačparac, R.; Martin, C. R.; Stupnišec-Lisac, E. *J. Electrochem. Soc.* **2000**, *147* (2), 548−551. Zhang, D. Q.; Gao, L. X.; Zhou, G. D. *Corros. Sci.* **2004**, *46* (12), 3031−3040. Sherif, E. M.; Park, S.-M. *Electrochim. Acta* **2006**, *51*, 6556−6562.

(5) Kawaquita, J.; Kobayashi, K. *J. Power Sources* **2001**, *101*, 47−52.

(6) Światowska-Mrowiecka, J.; Banaś, J. *Electrochim. Acta* **2005**, *50*, 1829−1840.

(7) Lebedeva, O.; Jungurova, G.; Zakharov, A.; et al. *J. Phys. Chem. C* **2012**, *116*, 22526−22531.

(8) Stypuła, B.; Banaś, J.; Starovicz, M.; et al. *J. Appl. Electrochem.* **2006**, *36*, 1407−1414.

(9) Di Francesco, F.; Calisi, N.; Creatini, M.; et al. *Green Chem.* **2011**, *13*, 1712−1717.